Docking studies, antitumor and antioxidant evaluation of newly synthesized porphyrin and metallo-porphyrin derivatives

Asmaa Ahmed[a,b], Walaa A. E. Omar[c,d*], Hala A. El-Asmy[b], Laila Abou-Zeid[e,f],

Ahmed A. Fadda[b]

[a]*Research Unit of Sustainable Chemistry, Faculty of Technology, P.O.Box 8000 FI-90014 University of Oulu − Finland.*

[b]*Chemistry Department, Faculty of Science, Mansoura University, 35516 Mansoura − Egypt*

[c]*Department of Basic Sciences, Faculty of Energy & Environmental Engineering, The British University in Egypt, El Sherouk City, P.O.Box 43, 11837 Cairo − Egypt. Walaa.Omar@bue.edu.eg*

[d]*Department of Engineering Sciences and Mathematics, Faculty of Petroleum and Mining Engineering, Suez University − Egypt.*

[e]*Pharmaceutical Organic Chemistry Department, Faculty of Pharmacy, Mansoura University, 35516 Mansoura − Egypt*

[f]*Pharmaceutical Chemistry Department, Faculty of Pharmacy, Delta University, 35516 Gamassa, Egypt*

Abstract

In this work we have synthesized a series of novel porphyrin derivatives, **1–5,** in high yields. The metal complexes of two of the newly synthesized porphyrin derivatives, **1a–d** and **2a–d,** have also been synthesized in high yields and characterized. In the synthesis of the new porphyrins and metallo-porphrins, we employed our reported strategy in which we utilized dimethyl formamide (DMF) as capping agent in the reaction of pyrrole with different hetero-aryl aldehydes. The new porphyrin derivatives are equipped with different

1

aromatic substituents and hetero-cycles at peripheral position. The structures of the new compounds were confirmed by elemental and spectral analyses. The geometry and magnetic properties of the new metalloporphyrins **1a–d** and **2a–d** have also been studied. Antioxidant and cytotoxic activities of the new compounds were evaluated and structure activity relationships were performed. Porphyrin derivatives **2a** and **4** showed exceptional antioxidant activity compared to ascorbic acid as a reference. While the derivatives **2, 3** and **5** exhibited very strong cytotoxic activity against two human cell lines, **HePG-2** and **MCF-7.** Docking for the most promising antioxidant porphyrins, **2a** and **4,** into the binding active site of antioxidant protein Human Peroxiredoxin (code: **1HD2**) has been carried out to detect the degree of recognition antioxidant activity. Molecular docking of the most cytotoxic active porphyrins, **3** and **5,** into the biding site of telomerase inhibitor enzyme has been carried out to assess the degree of recognition cytotoxic activity.

Key Words: Porphyrin; Capping mechanism; Metal Complex; Antioxidant; Antitumor; Docking Studies

1.   *Introduction*

Porphyrins and related tetrapyrrolic macrocyclic pigments are important heterocyclic compounds due to their wide chemical and biologically applications. They have been employed successfully in the areas of catalysis, medicine, and material science [1–4]. Additionally, metallo-porphyrins that coordinated to transition metal ions such as iron, cobalt and magnesium were able to perform a diversity of functions and applications [5–8].

Traditional strategies described by Rothemund and Alder's for porphyrins synthesis allowed the synthesis of limited structures of porphyrins through simple condensation between pyrrole and aldehydes and the yields were always very low (< 20%) [9–12]. The

difficulties of separation and the limited availability of suitable precursors are extra limitations during porphyrin traditional synthetic protocols. Since then, many modifications have been done to the Rothemund procedures in order to overcome the drawback accompanied the synthesis [13–16]. Among the considerable attempts dedicated to elaborate improved protocols for facilitating the synthesis of various useful porphyrin systems in satisfactory yields, our reported procedure has shown a considerable success. We succeeded to prepare a series of mesoporphyrins in high yields using DMF as a capping reagent [17–19].

Although many synthetic routes for certain porphyrins are available so far [14–17], it is still challenging to synthesize porphyrins bearing specific chemical groups in satisfactory yield (> 20%) [20–22]. Meso-substituted porphyrins have been considered as a key building block for porphyrin-based systems and molecular materials [3,13–15]. There is an increased interest in the development of meso-substituted porphyrin synthesis as they act as ligands for metal ions forming important metallo-porphyrins for therapeutic purposes [3, 23–27].

Porphyrin derivatives have been tested as sensitizing drugs for application in tumor diagnosis and treatments using photodynamic therapy (PDT) [24–29] and boron neutron capture therapy (BNCT) [30, 31]. In PDT and BNCT therapies, light and low energy neutrons are utilized for activation of a tumor-localized sensitizer, respectively.

In the above-mentioned therapeutical investigations, certain porphyrin derivatives undergo selective localization in tumor tissues depending on their affinity for carrier biomolecules and biological membranes [24–31]. Clearly, Positively charged porphyrins, such as tetra-(trimethylaminophenyl)- and meso-tetra(methylpyridyl)- porphyrins showed a strong interaction with the negatively charged groups of the biological targets , such as certain

proteins [32], RNA [33] and DNA [34, 35] , in addition to their effectiveness as photosensitizers for PDT [24–29, 32–34]. It is also observed that the number and distribution of the positive charges about the porphyrin macrocycle plays a very important role in its photodynamic efficacy [32, 34]. For example, amphiphilic porphyrin derivatives containing water-solubilizing groups, such as $-NMe_3^+$, showed an increasing photodynamic efficacy compared to hydrophilic macrocycles [33–35].

The free radical mediated peroxidation of membrane and oxidative damage of DNA were considered responsible for a variety of chronic health problems, such as cancer, antherosclerosis, neurodegenerative diseases, and aging [36]. Consequently, during the last years, many studies investigating biological attributes of different precursors, which include mainly antioxidant activity, have been reported [36, 37].

Apparently, studies related to the kinetics and mechanisms of natural antioxidants have shown that simple structural customization can lead to a noticeable enhancement in the antioxidative activity [38, 39]. An interesting example for such observation was resveratrol, an antioxidant component in red wine, in which chemical structure modification could efficiently improve its antioxidative activity and cytotoxicity against cancer cell [38].

Based on the above promising findings, we were motivated to use porphyrin as a basic nucleus to design more potential antioxidants and chemo preventive agents against cancer. The properties of porphyrin can also be modulated by the insertion of different metal ions such as copper, silver, nickel, and Zinc [40–43]. Therefore, we have also synthesized a novel series of porphyrin metal complexes in high yields and performed an in-vitro study of their protective effects. The new porphyrins have been prepared in high yields by using the previously reported modified one pot mixed solvent method in which DMF is used as

capping reagent [17–19]. All the synthesized compounds have been characterized and assessed for the antioxidant and antitumor activities. The geometry and magnetic interaction in the metal complexes have been also investigated using the electron spin resonance (ESR) technique.

2. Experimental Section

2.1. General remarks

^{1}H and ^{13}C-NMR spectra were measured on 300 MHz JOEL ECA-300 spectrometer, using DMSO or CDCl$_3$ as solvents and TMS as the internal standard, at the Micro analytical Center, Faculty of Science, Mansoura University. The IR spectra were recorded (KBr disk) on a Mattson 5000 FTIR Spectrometer at Faculty of Science, Mansoura University. Elemental analyses (C, H and N) were carried out at the Faculty of Science, Cairo University, the results were found to be in good agreement with the calculated values.

Ultraviolet spectra were recorded using Unicam UV2 UV/Vis spectrometer at the Microanalytical Unit, Faculty of Science, Mansoura University. Butylated hydroxyanisole (BHA) and *L*-ascorbic acid were purchased from Sigma-Aldrich Company. 2,2-Azo-bis-(2-amidinopropane) dihydrochloride (AAPH) and 2, 2-azino-bis(3-ethyl benzthiazoline-6-sulfonic acid) (ABTS) were purchased from Wako. All other chemicals were of analytical grade and purchased from sigma-aldrich, Germany.

2.2 Synthesis

2.2.1 Synthesis of porphyrin derivatives 1–5

General procedures for the synthesis of porphyrins 1–5:

A mixture of the appropriate aromatic aldehyde (0.72 mmol) and pyrrole (0.72 mmol) in DMF (15 ml) were placed into a 50 mL three-necked flask. The mixture was flushed with nitrogen gas for a couple of minutes and then heated to 100 ˚C for 10 min. *P*-toluene sulphonic acid (0.72 mmol, dissolved in DMF) was then added to the reaction mixture. The colorless mixture turned red over the next couple of minutes then heated at 150 ˚C for 1 hour. The reaction mixture was then cooled and poured over ice with stirring for 15 min. the residue was collected, dried under vacuum and purified by column chromatography using chloroform/hexane (1.5/1) as eluent.

Synthesis of 5,10,15,20- mesotetrakis[2,4- dichlorophenyl]-21,23H- porphyrin (1) (H₂mdcpp)

Dark brown color, yield 85%, m.p. 160 ˚C. IR (cm^{-1}): ν(N-H), 3279; ν(C=N), 1664; ν(C=C), 1584; ν(C-Cl), 784. ^{1}H-NMR (DMSO-d_6) (ppm): δ 2.27 (s, 1H, NH), 5.30 (d, 1H, 2 pyrrolic CH), 5.81 (d, 2H, 2 pyrrolic CH), 6.53 (d, 2H, 2 pyrrolic CH), 7.00 (d, 2H, 2 pyrrolic CH), 7.32 (d, 4H, Ar-H), 7.50 (d, 4H, Ar-H), 7.95 (s, 4H, Ar-H), 10.64 (s, 1H, NH). ^{13}C-NMR (DMSO-d_6) (ppm): δ 103.0, 120.5, 123.3, 125.0, 128.6, 130.5, 132.2, 135.7, 136.5, 137.7, 155.8, 181.1. UV-Vis. Spectrum: Λ_{max} = 413 nm.   Elemental Anal.: Calcd. C, 59.36; H, 2.49; N, 6.29; ($C_{44}Cl_8H_{22}N_4$); Found: C, 59.70; H, 2.53; N, 6.30%.

Synthesis of 5,10,15,20- mesotetrakis[4-N,N-dimethylaminophenyl]-21,23H- porphyrin (2) (mdmapp)

Dark violet color, yield 82%, m.p > 300˚C. IR (cm^{-1}): ν(NH), 3240; ν(CH₃), 2925; ν(C=N), 1659; ν(C=C), 1603. ^{1}H-NMR (DMSO-d_6) (ppm): δ 3.03 (s, 1H, NH), 3.90 (s, 24H, 4 N-(CH₃)₂), 5.31 (d, 2H, 2pyrrolic CH), 6.23 (d, 2H, 2pyrrolic CH), 6.46 (d, 2H, 2pyrrolic CH), 6.54 (d, 2H, 2pyrrolic CH), 6.95 (d, 8H, Ar-H), 7.25 (d, 8H, Ar-H), 10.23 (s, 1H, NH). ^{13}C-NMR (DMSO-d_6) (ppm): δ 106.4, 106.6, 107.4, 117.3, 128.6, 128.8, 124.4, 129.5, 132.2, 132.6, 149.3, 163.0, 167.6.

UV-Vis. Spectrum: $Λ_{max}$ = 421 nm. Elemental Anal.: Calcd. C, 79.37; H, 4.42; N, 14.26; ($C_{52}H_{50}N_8$); Found: C, 79.76; H, 4.42; N, 14.20%.

Synthesis of 5,10,15,20- mesotetrakis [4- carboxylic]-21,23H- porphyrin (3)

Deep green color, yield 75%, m.p > 300˚C. IR (KBr): $ύ$ /cm^{-1} = 3450 (OH), 3350 (NH), 1630 (C=N), 1570 (C=C), ^{1}H-NMR (DMSO-d_6) (ppm): $δ$ 2.30 (s, 1H, NH), 5.91 (d, 2H, 2 pyrrolic CH), 6.22 (d, 2H, 2 pyrrolic CH), 6.30 (d, 2H, 2 pyrrolic CH), 6.73 (d, 2H, 2 pyrrolic CH), 7.21 (d, 8H, Ar-H), 7.81 (d, 8H, Ar-H), 10.52 (s, 1H, NH), 10.56 (s, 1H, OH). UV-Vis. Spectrum: $Λ_{max}$ = 426 nm. Elemental Anal.; Calcd. for $C_{48}H_{30}N_4O_8$ (790), C 72.90; H 3.82; N 7.09%. Found:

C   72.52;   H   3.55;   N   7.50%.

Synthesis of 5,10,15,20- mesotetrakis [2-chloroquinolin-6-hydroxy-3-yl]-21,23H- porphyrin (4)

Porphyrin (**4**) was prepared according to the general procedure using the aldehydes (*A, 2-chloroquinoline-6-hydroxy-3-carboxaldehyde*) to give **4** as deep brown color, yield 64%, m.p >300˚C. IR (KBr): $ύ$ /cm^{-1} = 3340 (NH), 1630 (C=N), 1570 (C=C), 675 (C-Cl). ^{1}H-NMR (DMSO-d_6) (ppm): 6.20 (d, 2H, pyrrolic protons), 6.46 (d, 4H, pyrrolic protons), 7.22 (s, 4H, quinoline C_5-H), 7.33 (4H, quinoline C_7-H), 7.70 (d, 4H, quinoline C_8-H), 7.82 (d, 2H, pyrrolic protons), 8.24 (s, 4H, quinoline C_4-H), 8.80 (s, 1H, NH), 9.40 (s, 4H, 4OH), 9.92 (s, 1H, NH). UV-Vis. Spectrum: $Λ_{max}$ = 424nm. Anal. data for $C_{56}H_{30}Cl_4N_8O_4$ (1018), Calcd. C, 65.90; H, 2.96; 13.89; N, 10.98%. Found C, 65.88; H, 2.91; N, 10.99%

Synthesis of 5,10,15,20 tetrakis (4a, 10a-dihydro-10H-phenothiazin-3-yl) porphyrin (5)

Porphyrin (**5**) was prepared according to the general procedures using aldehyde (*B, 10, 10a-dihydro-4aH-phenothiazine-3 carbaldehyde*) to give **5** as deep blue color, yield 72%, m.p >

300˚C. IR (KBr): ὐ /cm^{-1} = 3340 (NH), 1630 (C=N) , 1570 (C=C), ^{1}H-NMR (DMSO-d_6) (ppm): 3.03 (s, 1H, NH), 6.66- 7.51 (m, 29H, Ar-H) 8.57 (s, 1H, NH) ^{13}C-NMR (DMSO-d_6) (ppm) d: 114.4, 115.3, 121.7, 122.5, 125.6, 126.2, 127.0, 127.1, 127.2, 127.5, 128.2, 128.7, 129.2, 134.9, 137.2, 142.0. UV-Vis. Spectrum: $ʎ_{max}$ = 422 nm. Anal. Calcd. for $C_{68}H_{50}N_8S_4$ (1106). C, 73.75; H, 4.55; N, 10.12%. Found C, 73.70; H, 4.50; N, 10.10%.

Synthesis of aldehydes, 2-chloroquinoline-6-hydroxy-3-carboxaldehyde (A) and 10, 10a-dihydro-4aH-phenothiazine-3 carbaldehyde (B):

Synthesis of 2-chloroquinoline-6-hydroxy-3-carboxaldehydes (A)

Dimethylformamide (9.13 g, 9.6 mL, 0.125 mol) was cooled to 0 ˚C in a flask equipped with dry tube and phosphoryl chloride (53.7 g, 32.2 mL, 0.35 mol) was added drop wise with stirring. To this solution was added the *N*-Phenyl-acetamide (0.05 mol). After 30 min the solution was heated under reflux for 15 hrs in a water bath. The reaction mixture was poured onto ice-water (300 ml) and stirred for 30 min at 0–10 ˚C. The separated solid material was filtered off and washed with water. The combined filtrate was adjusted to pH 9 with aqueous sodium hydroxide, chloroform (200ml) was added and the mixture was stirred for 30 min and then separated. The aqueous phase was extracted further with chloroform, combined organic layer was dried with magnesium sulphate and evaporated to give oil which was treated with HCl and extracted further with chloroform, the organic layer to give the corresponding aldehyde (**A**). Deep yellow, yield 93%, m.p =185 ˚C. IR (KBr): ὐ /cm^{-1} = 3400 (OH), 1730 (C-C=O), 1630 (C=N), 695(C-Cl). ^{1}H-NMR (DMSO-d_6) (ppm): δ 7.26 (s, H$_4$), 7.47 (d.d, H$_7$) (J$_{7,8}$ = 9), 7.87 (d.d, H$_8$) (J$_{8,7}$ = 2) 8.78 (s, H$_5$), 9.22 (s, CHO), 9.78 (s, 1H, OH). Anal. Calced for $C_{10}H_6NO_2Cl$ (207), C, 57.85, H, 2.91, N, 6.75% found C, 57.80; H, 2.89; N, 6.68 %.

Synthesis of 10, 10a-dihydro-4aH-phenothiazine-3 carbaldehyde (B)

Aldehyde (B) was synthesized following the general procedures used for the synthesis of aldehydes (A) starting from the base phenothiazine. Off-white powder, yield 80%, m.p 175–185 ˚C. IR (KBr): υ /cm^{-1} = 3340 (NH), 1730 (C=O), 1570 (C=C), ^{1}H-NMR (DMSO-d_6) (ppm): 6.88-7.51 (m, benzene ring), 8.59 (s, 1H, NH), 8.70 (s, 1H, CHO) Anal. Calcd. for $C_{13}H_{11}NOS$ (229). C, 68.09; H, 4.84; N, 6.11%. Found C, 68.00; H, 4.79; N, 6.01%.

2.2.2 Synthesis of the new metalloporphyrins 1a–d and 2a–d

General procedure:

The metal complexes from the free porphyrins **1** and **2** have been prepared using the following routes:

Route 1: The complexes were prepared by heating a mixture of porphyrin **1** or **2** (0.25 mmol) dissolved in 10 mL ethanol and the metal salt (0.25 mmol of $CuCl_2.2H_2O$, $VOSO_4.H_2O$, $AgNO_3$ or K_2PdCl_4) dissolved in 10 mL H_2O under reflux for 6–8 hours. After cooling to room temperatures, the precipitate was filtered off, washed with ethanol, diethyl ether and dried.

Route 2: The proper aldehyde (0.01 mol) was dissolved in DMF (50 mL) and p-toluen sulfonic acid (0.01 mol) was added. Pure pyrrole (0.01 mol) was then added dropwise. The mixture was stirred under argon for one hour followed by the addition of 2.5 equiv. of the proper metal salt. The whole reaction mixture was then refluxed for 8 hours in air. The solvent was removed under vacuum and the crude product was washed with water, dried and purified by flash chromatography over silica gel using chloroform as eluent.

[Cu(mdcpp)].3H₂O (1a):

Dark green ppt. Yield: (85%). IR (cm^{-1}): ν(C=N), 1604; ν(C=C), 1576; ν(C-N), 1335; ν(Cu-N), 502. UV-visible (nm): 536, 640. μ_{eff}= 1.9 B. M. Elemental Anal.: Calcd. C, 52.4; H, 2.6; N, 5.6; (C$_{44}$Cl$_8$CuH$_{26}$N$_4$O$_3$); Found: C, 52.7; H, 2.9; N, 5.52%.

[VO(mdcpp)] (1b):

Dark red ppt. Yield: (83%). IR (cm^{-1}): ν(C=N), 1621; ν(C=C), 1598; ν(C-N), 1349; ν(V-N), 510. UV-visible (nm): 302, 410, 648. μ_{eff}= 2.1 B. M. . Elemental Anal.: Calcd. C, 55.3; H, 2.1; N, 5.9; (C$_{44}$Cl$_8$H$_{20}$N$_4$OV); Found: C, 55.2; H, 2.0; N, 5.7%.

[Ag$_2$(mdcpp)(H$_2$O)$_2$] (1c):

Dark violet ppt. Yield: (87%). IR (cm^{-1}): ν(C=N), 1634; ν(C=C), 1580; ν(C-N), 1353; ν(Ag-N), 530. ^{1}H-NMR (DMSO-d_6) (ppm): δ 5.56 (d, 1H, 2 pyrrolic CH), 5.90 (d, 2H, 2 pyrrolic CH), 6.63 (d, 2H, 2 pyrrolic CH), 7.97 (d, 2H, 2 pyrrolic CH), 7.32 (d, 4H, Ar-H), 7.56 (d, 4H, Ar-H), 8.31 (s, 4H, Ar-H). UV-visible (nm): 306, 416. Elemental Anal.: Calcd. C, 46.3; H, 2.1; N, 4.9; (Ag$_2$C$_{44}$Cl$_8$H$_{24}$N$_4$O$_2$); Found: C, 46.0; H, 1.9; N, 4.6%.

[Pd(mdcpp)](1d):

Dark blue-black ppt. Yield: (84%). IR (cm^{-1}): ν(C=N), 1619; ν(C=C), 1584; ν(C-N), 1378; ν(Pd-N), 510. ^{1}H-NMR (DMSO-d_6) (ppm): δ 5.33 (d, 1H, 2 pyrrolic CH), 5.87 (d, 2H, 2 pyrrolic CH), 6.51 (d, 2H, 2 pyrrolic CH), 6.96 (d, 2H, 2 pyrrolic CH), 7.35 (d, 4H, Ar-H), 7.55 (d, 4H, Ar-H), 8.11 (s, 4H, Ar-H). UV-visible (nm): 347, 460, 994.4. Elemental Anal.: Calcd. C, 53.1; H, 2.0; N, 5.6; (C$_{44}$Cl$_8$H$_{20}$N$_4$Pd); Found: C, 52.9; H, 1.8; N, 5.3%.

[Cu(mdmapp)].4H2O (2a):

Red bloody ppt. Yield: (82%). IR (cm^{-1}): ν(CH$_3$), 2934; ν(C=N), 1659; ν(C=C), 1590; ν(C-N), 1318; ν(Cu-N), 540. UV-visible (nm): 318, 414, 470. μ_{eff}= 1.6 B. M. Elemental Anal. Calcd. C, 67.7; H, 6.1; N, 12.2; (C$_{52}$CuH$_{56}$N$_8$O$_4$); Found: C, 67.7; H, 5.9; N, 11.9%.

[Ni(mdmapp)(H2O)2].3H2O (2b):

Dark green ppt. Yield: (87%). IR (cm^{-1}): v(CH$_3$), 2934; v(C=N), 1659; v(C=C), 1590; v(C-N), 1335; v(Cu-N), 540. UV-visible (nm): 318, 383, 438, 538, 799. μ_{eff}= 3.23 B. M. Elemental Anal.: Calcd. C, 66.8; H, 6.2; N, 12.0; (C$_{52}$H$_{58}$N$_8$NiO$_5$); Found: C, 66.5; H, 6.3; N, 11.8%.

[Ag$_2$(mdmapp)(H$_2$O)$_2$] (2c):

Dark blue ppt. Yield: (87%). IR (cm^{-1}): v(CH$_3$), 2936; v(C=N), 1600; v(C=C), 1573; v(C-N), 1320; v(Ag-N), 520. ^{1}H-NMR (DMSO-d_6) (ppm): 3.92 (s, 24H, 4 N-(CH$_3$)$_2$), 5.32 (d, 2H, 2pyrrolic CH), 6.21 (d, 2H, 2pyrrolic CH), 6.46 (d, 2H, 2pyrrolic CH), 6.59 (d, 2H, 2pyrrolic CH), 6.83 (d, 8H, Ar-H), 7.29 (d, 8H, Ar-H). UV-visible (nm): 306, 401, 471. Elemental Anal. Calcd. C, 62.3; H, 5.2; N, 11.2; (Ag$_2$C$_{52}$H$_{56}$N$_8$O$_2$); Found: C, 62.0; H, 5.1; N, 11.0%.

[Pd(mdmapp)].2H$_2$O (2d):

Dark brown ppt. Yield: (82%). IR (cm^{-1}): v(CH$_3$), 2934; v(C=N), 1659; v(C=C), 1590; v(C-N), 1335; v(Cu-N), 540. ^{1}H-NMR (DMSO-d_6) (ppm): δ 3.72 (s, 24H, 4 N-(CH$_3$)$_2$), 5.29 (d, 2H, 2pyrrolic CH), 6.22 (d, 2H, 2pyrrolic CH), 6.44 (d, 2H, 2pyrrolic CH), 6.55 (d, 2H, 2pyrrolic CH), 6.87 (d, 8H, Ar-H), 7.32 (d, 8H, Ar-H). UV-visible (nm): 311, 437, 502. 928.4 Elemental Anal.: Calcd. C, 67.2; H, 5.6; N, 12.1; (C$_{52}$H$_{52}$N$_8$O$_2$Pd); Found: C, 67.2; H, 5.5; N, 12.0%.

2.3 Biochemical assays (Antioxidant properties, Cytotoxicity and antitumor assay)

2.3.1 Antioxidant properties

Free radical scavenging activity of all the new compounds was evaluated by measuring their ability to neutralize DPPH and OH radicals. The DPPH (2,2-diphenyl-1-picrylhydrazyl) assay and hydroxyl-radical scavenging assays were applied as previously reported [17, 18].

2.3.2 Cytotoxicity and antitumor assay

Cytotoxicity and antitumor assay have been carried out according to the previously reported procedures [17, 18].

2.4 Docking studies

2.4.1 Docking of antioxidant active porphyrin derivatives 2a and 4

All computational modeling were conducted with **Schrödinger** Suite 2015 (**Schrödinger**, LLC) that were run on dual core PC [44].

The newly synthesized compounds were comparatively evaluated in terms of their binding mode to the Human Peroxiredoxin 5, antioxidant enzyme (1HD2) pocket. Compounds **2a** and **4** showed potential antioxidant activity therefore they were considered for further molecular modeling study in order to explore their recognition profile at the human 1HD2 binding active site.

- Preparation of enzyme:

The starting coordinates of the X-ray crystal structure of Human Peroxiredoxin in complex with the BEZ 201A (PDB code: 1HD2) that retrieved from the RCSB Protein Data Bank of Brookhaven National Laboratory [45]

- Preparation of tested porphyrin

Molecular docking for compounds **2a** and **4** into the biding site of oxidase enzyme was performed using the **Schrödinger** Suite 2015 (**Schrödinger**, LLC) [44]. The three-dimensional structures of both compounds were constructed using building module. Gasteiger–Hückel charges of ligands were assigned. AMBER with 100 iterations was utilized for energy minimization. The active site of the protein was defined to contain residues within a 10.0-Å radius around any of the inhibitor atoms. All hydrogens were added and the enzyme structure was exposed to a refinement protocol in which the

constraints on the enzyme were systematically eliminated and minimized until the RMS gradient was 0.01kcal/mol Å. The conformer with the lowest energy, the "global-minima," was pre-positioned using the crystal structure ligand "BEZ 201A" as a template at the enzyme-binding pocket.

2.4.2 Docking antitumor active porphyrin derivatives 3 and 5

Molecular docking of compounds (**3 and 5**) into the biding site of telomerase was explored using **Schrödinger** Suite 2015 (**Schrödinger**, LLC). The three-dimensional structures of the aforementioned compounds were constructed using Chem. Draw 3D Ultra 11.0 software. Using compute module to perform Gasteiger–Hückel, charges of ligands were assigned. Porphyrin derivatives, **3** and **5,** were energetically minimized by using AMBER with 100 iterations and minimum RMS gradient of 0.10. The template (PDB code: 2A5R) was obtained from the RCSB Protein Data Bank.

- Preparation of the enzyme

The starting coordinates of the X-ray crystal structure of complex of tetra(4-*n*-methylpyridyl) porphin with monomeric parallel-stranded DNA Tetraplex (PDB code 2A5R: in complex with the POH 25A) that retrieved from the RCSB Protein Data Bank of Brookhaven National Laboratory [46]

- Preparation of tested porphyrin

Molecular docking of compounds (**3** and **5**) into the binding site of telomerase inhibitor enzyme was investigated using the **Schrödinger** Suite 2015 (**Schrödinger**, LLC). The three-dimensional structures of the aforementioned compounds were constructed using building module. Gasteiger–Hückel charges of ligands were assigned. They were energetically minimized by using AMBER with 100 iterations. The active site of the protein was defined to contain residues within a 10.0-Å radius around any of the inhibitor

atoms. All hydrogens were added and the enzyme structure was exposed to a refinement procedure in which the constraints on the enzyme were gradually eliminated and minimized until the RMS gradient was 0.01kcal/mol Å. Conformer with the lowest energy, the "global-minima", was pre-adjusted using the crystal structure ligand "**POH 25A**" as a template at the enzyme-binding pocket.

3. Result and Discussion

3.1 Synthesis and characterization

This work reports the synthesis of new porphyrin derivatives including the free base compounds **1–5** (scheme 1) and metal complexes **1a–d**, **2a–d** (Scheme 2) which were evaluated as antitumor and antioxidant agents.

<scheme 1>

<scheme2>

3.1.1 Synthesis and characterization of the free porphyrins 1–5:

The low yields (6–20%) in porphyrin chemistry is a persistent obstacle so far, although the continuous advancement in the porphyrin synthesis [20–22]. Recently, Fadda *et al* [17, 18] developed a synthetic method that gives 80–90% yield with minimal chromatography. We used the capping mechanism to prevent the pyrrole polymerization process. Dimethylformamide (DMF) was used as a solvent and capping reagent (**Scheme 3**). The DMF-pyrrole intermediate reacts with more pyrrole to keep constructing the corresponding porphorengon, and the DMF molecule would act as good leaving group in each time pyrrole is added [17–19].

<Scheme 3>

Our reported strategy facilitated the synthesis of various derivatives of porphyrin and metalloporphyrin in high yields [17, 18]. In this work, we were able to obtain the free-base prophyrins **1–5** in high yields (64–85%). The newly synthesized porphyrins were well characterized by spectral data. In the ^{1}H-NMR spectra, porphyrin derivatives **1–5** showed two sets of doublets between δ 5.00 and 8.00 ppm that corresponds to the pyrrolic CH protons which is different from the signals for porphyrins normally found above δ 8.00 ppm. This shift in peaks position may be related to the increased shielding of the pyrrolic protons resulting from the interference of electron delocalization within the macrocycle.

^{1}H-NMR of porphyrin **1** showed a singlet signal at δ 10.64 ppm that corresponds to the N-H proton, two doublet signal at δ 7.32 and 7.22 ppm and a singlet signal at δ 7.48 due to the deshielded aromatic protons, in addition to the doublets signals at δ 6.24, 6.38, 6.44 and 7.84 ppm characterizing the pyrrolic protons.

^{1}H-NMR of porphyrin **2** showed a characteristic singlet signal at δ 10.23 ppm corresponding to the N-H proton. Aromatic protons displayed a characteristic two doublets due to (AB system) at δ 6.77 and 7.16 ppm, while pyrrolic protons appeared as doublets at δ 6.24, 6.38, 6.44, and 7.84 ppm. The singlet signal for ($-N(CH_3)_2$) protons appeared at δ 3.02 ppm.

^{1}H-NMR of porphyrin **3** showed a characteristic singlet signal at δ 12.71 ppm due to carboxylic proton and another singlet signal at δ 10.52 ppm that corresponds to the N-H proton. The aromatic system represented as two doublets at δ 7.83 and 7.55 ppm due to "AB system". Pyrrolic protons appeared at its normal position at δ 6.00–7.50 ppm as doublets.^{13}C-NMR displayed an obvious signal at δ 167.6 ppm characterizing the carbonyl carbon.

^{1}H-NMR of porphyrin (**4**) displayed a singlet signal at δ 9.92 ppm due to -NH proton, a singlet at δ 9.40 corresponding to the O-H group, in addition to pyrrolic and quinolinic protons at the range δ 6.20–8.40 ppm.

^{1}HNMR of porphyrin (**5**) displayed a singlet signal at δ 8.57 ppm due to N-H protons, in addition to a complex pattern of multiplet signals due to pyrrolic and aromatic protons at δ 5.60- 7.80 ppm.

3.1.2 Synthesis and characterization of *metallo*porphyrins 1a–d and 2a–d

Recently, the biochemical and photo-electro properties of porphyrin have attracted a growing interest. Substituted metalloporphyrins are now playing crucial roles in the fields of iatrology [47], medicinal chemistry, [48–50], analytical chemistry [49] and electronic devices [13–15, 51, 52]. It has been observed that when a porphyrin complex is applied in the natural enzyme peroxidase, the dioxygen gets activated under mild conditions therefore, porphyrin complexes with various metal ions have received much attention as antioxidants [53].

Metalloporphyrins were synthesized by the classical Alder two-step strategy, which involves the reaction of the free base porphyrin with the proper metal salt in refluxing DMF [12]. The yields of metalloporyphrins obtained by this method were unsatisfactory ($< 20\%$) which is apparently a result of the long reaction time and pyrrole polymerization. On the other hand, in the present work, one-pot reaction method with DMF as a capping agent was proved to be very successful. The later strategy has the advantages of the short reaction time, simple work up and higher yield of the porphyrin complexes [40, 41]. In the one-pot reaction method, pyrrole, a proper aldehyde and the metal salt were mixed together and refluxed for a reasonable short time to produce a variety of metalloporphyrins in high

yields. In this work, the addition of DMF as a capping reagent during the one pot synthesis for the metalloporphyrins **1a–d** and **2a–d** increased the yield dramatically (82–87%) compared to the two-steps method in which the free porphyrin has to be prepared before the following step in which the metal ion is added.

Cu(II), Pd(II), Ag(I) and VO^{2+} porphyrin metal complexes showed exceptional properties for medicinal and biological applications [47–50]. While Nickel porphyrin complexes have been employed successfully in catalytic reactions [54]. Therefore, in the synthesis of the new complexes **1a–d** and **2a–d,** metal II salts of Cu(II), Ag(I), Ni(II), VO^{2+}, and Pd(II) have been used along with the pyrrole and the proper aldehydes (Scheme **2**).

The structures conformation of the matal complexes **1a–d** and **2a–d** were examined by IR spectroscopy and compared to that of the free porphyrins, 5,10,15,20- mesotetrakis [2,4-dichlorophenyl]-21,23H- porphyrin (**1**) and 5,10,15,20- mesotetrakis[4-N,N-dimethylaminophenyl]-21,23H- porphyrin (**2**). The IR absorption frequencies for the complexed porphyrins **1a–d** and **2a–d** showed two main differences than the free porphyrins **1** and **2**. Firstly, The N-H bond stretching and bending frequencies of free porphyrins located at ~3,300 cm^{-1} and ~960 cm^{-1}. Insertion of the metal ion into the porphyrin resulted in the disappearance of the N-H group and alternatively, the band characteristic for the functional groups of M-N bond appeared at ~1,000 cm^{-1}. This obviously confirmed the formation of metalloporphyrin derivative. Secondly, As the coordination between the nitrogen and the metal ion reduces the electron density in the azomethine link, the band at ~1664, 1659 cm^{-1} corresponding to the $v(C=N)$ group in the free porphyrin is shifted in the complexes towards lower wave number values ~ 1600–1630 cm^{-1}. The bands observed in the region around 1310–1370 cm^{-1} are attributed to υ (C-N) stretching vibrations in the complexes. This value is less than the value of υ (C-N)

17

stretching in ligands, which appears at 1383 and 1355 cm^{-1}, respectively. This decrease by 55–20 cm^{-1} in the metalloporphyrin is probably due to the increase in electron density of azomethine (C-N) bond due to π–electron delocalization from the metal to the nitrogen atom and resonance interaction with porphyrin ring. Therefore, it can be inferred that **1**$^{--}$ and **2**$^{--}$ acted as bi-negative tetradentate ligands, coordinating the metal ions through the azomethine nitrogen and the deprotonated imine nitrogen centers forming four six-membered rings. Moreover, the several bands at 550–500 cm^{-1} due to ν (M-N) stretches were observed in the IR spectra of the complexes [55].

The ^{1}H-NMR spectroscopic data for the complexes **1c, 1d, 2c and 2d** in DMSO-d_6 are reported in the experimental section. The ^{1}H-NMR spectra for metalloporphrins **1c, 1d, 2c and 2d** confirmed the complexation of the free porphyrins **1** and **2** with the proper metal ions. The spectra of free porphyrin **1 and 2** showed sharp singlet signals characterizing the NH proton at δ 10.64 and δ 10.23 ppm, respectively. In the spectra of complexes **1c, 1d, 2c and 2d**, The NH signals disappeared due to the replacement of the imine proton of the free porphrins by the metal ions, which confirms the formation of complexes **1c, 1d, 2c and 2d**. On the other hand, the signals for pyrrolic -CH are slightly shifted to downfield due to the complexation of 1^{--} and 2^{--} through the deprotonated imine nitrogen and the metal centers [55].

3.2 Electronic and geometrical studies of metalloporphyrins 1a–d and 2a–d

3.2.1 Magnetic and electronic spectra for complexes 1a–d and 2a–d

The electronic spectra of the complexes **1a–d** and **2a–d** in DMSO contain intense bands. The bands between 430–900 nm are resulting from ligand-to-metal charge-transfer (LMCT) transitions while weaker bands are assigned to d–d transitions. The intra-ligand charge transfer (n $\rightarrow$ π* and π $\rightarrow$ π*) appeared as transitions below 430 nm. The electronic

spectra of the diamagnetic Pd (II) complexes (**1d**, **2d**) exhibit bands near 465 and 340 nm due to $^1A_{1g}{\rightarrow}^1B_g$ and $^1A_{1g}{\rightarrow}^1E_g$ transitions, respectively, which relevant to a square-planar configuration [56]. The magnetic moment of $[Ni(mdmapp)(H_2O)_2]$ **2b** is 3.24 BM assigned for octahedral structure with ^3A_2g ground term [56, 57]. Interestingly, Its electronic spectrum shows a broad band at 799 nm is assigned to the $^3A_2g{\rightarrow}^3T_1g$ (F) (ν_2) transition [57]. The electronic spectra of [Cu(mdcpp)] **1a** and [Cu(mdmapp)] **2a** exhibit bands near 640 nm assigned to $^2T_2g{\rightarrow}^2Eg$. The band positions with magnetic moments of 1.9 and 1.6 BM are designated to a square-planar geometry [56, 57]. The porphyrins in plane geometry is crucial factor of Cu(II) square planar geometry.

3.2.2 Electron spin resonance (ESR) spectra of the Cu(II) and VO(IV) complexes

ESR spectrum of the complexes **1a, 1b** and **2a** were recorded in the solid state in order to identify the stereochemistry and the site of the metal-ligand bonding as well as the magnetic interaction in the metal complexes. Generally, the mononuclear oxo-vanadium (VO^{+2}), (S = 1/2, I = 7/2) has a characteristic octet ESR spectrum showing the hyperfine coupling owing to ^{51}V nuclear magnetic moment [58]. In comparison with other reported ESR spectrum of VO^{2+} [59], Compound **1b** shows a broad single line with poorly resolved eight-line pattern. Specifically, in the powder sample, the spectrum shows parallel and perpendicular features corresponding to axially symmetric anisotropy with poorly resolved sixteen-lines hyperfine splitting which confirms the interaction between the electron and the vanadium nuclear spin (I = 7/2) [60]. The spin Hamiltonian parameters for the complex are calculated as $g_{\parallel}$ = 1.93, $g_{\perp}$ =1.96 and the hyperfine coupling $A_{\parallel}$ = 195×10^{-4} (cm^{-1}), $A_{\perp}$

= 55. The ESR parameters indicate that the unpaired electron (d^1) of **1b** complex is present in the d_{xy} orbital with square-pyramidal geometry [65, 66]. The values obtained for this complex is in complete agreement with those reported for VO^{2+} square pyramidal geometry

[61]. The spectra of the Cu (II) complexes **1a**, **2a** at 300 K show a strong isotropic absorption band in the high field area due to the tumbling motion of the molecules. These complexes at 77K show four well-resolved peaks of low intensities in the low field area and one single intense peak in the high field area. In square planar complexes, the unpaired electrons are in the d_{x2-y2} orbital and ^2B_1g is the ground state with the $g_\parallel > g_\perp$. Based on the detected values, it is clear that $g_\parallel > g_\perp$ (2.37 > 2.08), which confirms square planar geometry of the complexes. Also, No band for Cu–Cu interaction was observed which indicates the mononuclear Cu (II) [62].

3.3 Pharmacology of porphyrins

3.3.1 Antioxidant activity:

The newly synthesized compounds **1–5**, **1a–d, 2a, 2c** and **2d** were evaluated as antioxidant agents using DPPH assay at different concentrations of 5 mg/mL of each tested sample [63]. Ascorbic acid was used as a reference drug. The radical scavenging activity was determined for the synthesized compounds using 1,1-dipheny l-2-picrylhydrazyl radical (DPPH$^\bullet$) as a stable radical organic compound and its oxidative method is widely used in the determination of the capacity of free radical scavengers or the capacity of hydrogen donors following *in vitro* assay. The type of antioxidant tests is suggested for the compounds containing reactive nitrogen, oxygen and carbon atom species. The mechanism of action of antioxidant tests as reported previously [64] initiated by the transfer of hydrogen atom, single electron and followed by proton transfer.

From the results of inhibitive concentrations (IC$_{50}$) in **Table 1**, compounds **2a** and 4 are the most potent antioxidant compounds compared to the results of ascorbic acid. On the other hand, compounds **5**, **2c**, **2d**, **1a** and **1b** exhibited good antioxidant activity, while,

compounds **2**, **3**, **1c** and **1d** have moderate activity. Compound **1** have the highest value of IC_{50} = 1.760 mg/ mL and considered as the less potent antioxidant agent.

In addition, the changes in the free radical scavenging capacity of the test compounds and their metal complexes depending on the inhibition percent are shown in **Table 1**.

3.3.2 *Structure activity relationship (SAR) for the antioxidant activity*

The metal complexes **1a–d** showed an enhanced antioxidant activity with lower values of IC_{50} compared to porphyrin **1**. Similarly, complexes **2a**, **2c** and **2d** showed an improved oxidative capacity compared to the free porphyrin **2**. The scavenging activity of the formed complexes, in general, is significantly higher than that of the corresponding free ligands, indicating that the formed complexes are stronger than free radical scavengers [65].

It was noticed that compound **2** is more potent antioxidant agent compared to compound **1**. Moreover the presence of electron donating substituents on aromatic ring increases the antioxidant activity [66] and the electron withdrawing substituents decreases it. Chlorine atoms have strong electron withdrawing character and are highly electronegative atoms. So, compound **1** has eight chlorine atoms, which actually decrease the antioxidant activity. In addition compound **3**, which has four carboxylic groups (strong electron attracting group) also decrease the antioxidant activity (Table 3). On the other side, compound **2** which contain four $-N(CH_3)_2$ groups that have electron donating character enhance antioxidant capacity of compound **2** compared to compound **1**.

The obtained results showed that compounds **2a** and **4** have the ability to trap the free radicals and displayed antioxidant capacity higher than ascorbic acid (**Vitamin C**). The copper (II) complex **2a** showed high antioxidant activity than its corresponding ligand, this result is in a great agreement with previously reported work [67]. Moreover, the presence

of four hydroxy groups in compound **4** as phenolic substituents increase the antioxidant capacity.

The order of free radical scavenging capacity of the tested compounds and their complexes as followed: **2a** > **4** > **Vit. C** > **5** > **2c** > **2d** > **1b** > **1a** > **2** > **1d** > **1c** > **3** > **1**.

The oxidative potentials of the synthesized compounds are related to the presence of compounds capable of exerting impact by breaking the chain of free radicals through hydrogen atoms donation [62]. Consequently, the obtained antioxidant results from this study prolong a link with the use of these compounds in the pathological diseases treatment, which arise from oxidative stress.

<Table1> and <Figure 1>

3.3.3 Cytotoxicity (anticancer screening):

Cytotoxicity studies of the newly synthesized compounds were performed against two mammalian cancer cell lines, HepG2 and MCF-7 cells. The evaluation process was carried out according to the previously reported work [17]

The newly synthesized compounds **1–5, 1a–d** and **2a–d** were screened for cytotoxic activity (**Table 2**) against HepG2 (hepatoma cells or human liver hepato carcinoma cell line) and MCF-7 cells (human breast adenocarcinoma cell line). The results were expressed as growth inhibitory concentration (IC_{50}) values, which represent the compounds concentrations required to produce a 50% inhibition of cell growth after 72 hours of incubation, compared with untreated controls (Table 2, Fig. 2). Generally, All the tested compounds showed a cytotoxic activity that ranged from very strong to weak activity. Compound **5** showed an IC_{50} value (5.56 ± 0.4 µg/mL) that is very similar to DOX as a standard for the two used cell lines. The most promising values were observed from

22

compounds **2** and **3** (very strong activity) with an IC_{50} value of 5.52 ± 1.1 and 6.34 ± 0.7 µg/mL for HePG-2 cell line, respectively. Compounds 5, 2 and 3 exhibited very strong activity with an IC_{50} value of 4.28 ± 0.3, 8.83 ± 1.2 and 7.51 ± 0.5 µg/mL for MCF-7 cell line, respectively. Compounds **1a, 1b, 2b and 4** exhibited strong activities for both cell lines. Compounds **1, 1d, 2a, 2c, 2d** have moderate cytotoxic activities against the same cell lines.

<center>**<Figure 2 >, < Table 2>**</center>

3.3.4 Structure activity relationship (SAR) from cytotoxicity studies:

The cytotoxic activity of the new porphorins towards different cell lines depends the following: Firstly, the intermolecular hydrogen bonds formed between the porphorin derivatives and DNA bases. Secondly, the positive charges on the tested porphyrins that are attracted to the negative charges on the cell wall. By comparing the experimental cytotoxic data of the new compounds to their structures, the following SAR was inferred: Compounds **5, 3 and 2** have exceptional strong activities, this can be attributed to the substituents, $-NH$, $-N(CH_3)_2$ and $-COOH$ which may undergo addition to any unsaturated moiety in DNA or form hydrogen bonds with any of the nucleo-bases of the DNA and causes its damage .

Compounds **1a and 1b** showed strong activity towards the tested cell lines due to the presence of strong electron attracting chlorine atoms which caused the molecules to be positively charged resulting in electrostatic attraction with the DNA nucleobases. For compound **4,** the strong activity is probably caused by chlorine atom as electron withdrawing substituent and one hydroxyl group which may also be added to any

unsaturated moiety in DNA or forming hydrogen bond with either one of the nucleobases of the DNA and causes it damage.

<center>**<Table2>, <Figure 2>**</center>

3.4 Molecular Docking Studies:

3.4.1 Docking studies for the new porphyrins 2a and 4

Free radical-scavenging activity properties using the 3-D crystallographic peroxiredoxin 5 (PRDX5) were carried out to explore the new porphyrins recognition in the active site as potential antioxidant.

As porphyrins **2a** and **4** showed the most powerful antioxidant activities, docking of the of **2a** and **4** into the binding active site of antioxidant protein Human Peroxiredoxin (code: 1HD2) has been conducted to check the degree of recognition antioxidant activity. The tested compounds, **2a** and **4** were prepared by partial charges and optimal minimizations using the compute module of MOE.

Compound **2a** and **4** showed proper and promising antioxidant activity by proper recognition at the binding active site of Human Peroxiredoxin protein. By studying the binding behavior of the new compounds relative to the antioxidant; BEZ 201A reference ligand that docked at the 1 HDC complex, it was found that hydrogen bonds, and hydrophobic interactions formed with the surrounding amino acids are used to predict their binding modes. This active pocket consisted of conserved amino acid residues including Thr44, Gly46, Cys47 and Arg127 that play fundamental roles in recognition of the docked compounds by hydrogen bonding interaction and hydrophobic interactions.

<center>24</center>

Metallo complex compound **2a** is hocked by bifurcated two hydrogen bonds between the conserved Arg127 residue and the two *N*-pyrrols that are facing Arg127. A third heterocyclic pyrrole ring showed π-π stacking interaction with Arg127.

Docking studies of compound **4** revealed that the crucial amino acid Arg127 played an important role in recognition of the ligand by forming strong hydrogen bonds between *N*-pyrrole and *N*-arginine. There are also hydrogen bonds that formed between hydroxy aliphatic function group and the conserved amino acid, Val75. Moreover, the amino group of the key amino acid, Arg127, which is one of conserved residues at the binding pocket, showed proper complementarity with the *N*-pyrrol atom in addition to the π-π stacking interaction between Arg127 and the heterocyclic pyrrole ring (Fig.3).

<**Figure** 3>

3.4.2 Porphyrin derivatives and their interaction with Telomerase (Telomerase inhibition activity):

The availability of a high-resolution crystallographic structure of the human telomerase enzyme facilitated the research considering the small molecules with potential telomerase inhibition activity that brings to light selective and safe cure of cancer. Telomerase becomes one of the competitive targets in the field of cancer treatment. Additionally, it plays a unique anti-aging role.

In this study, we aimed to find efficient G-quartets ligands that would be able at the same time to discriminate between different forms of nucleic acids in order to be selective as telomeric DNA. The binding of porphyrins allows them to match perfectly large planar surfaces of G-quartets.

<**Figure 4**>

25

G-quartet consists of four guanine bases, so its square is twice as large as the square of the base pair. Large porphyrin ligands perfectly overlap with G-quartets and professionally expressed proper quadruplex selectivity.

The standard porphyrin ligand, **POH 25A,** that aligned in the G-quartet 2A5R protein showed appropriate recognition with the ceiling DG-4 and DG-8 bases by forming π-π stacking interactions with the two pyridine heterocyclic rings back protruded from the minor groove. In the meantime, DG-13 and DG-17 bases in the major groove flooring showed amplifying recognition with both pyridine heterocyclic rings exposed from the major groove showed in **figure 5**

<Figure 5>

- Docking studies of Compound 3:

Telomerase and compound **3** have strong complementarities as it sandwiched between the roof and floor of the major groove of telomeric DNA as the reference ligand **POH 25A**. In comparative docking studies where POH 25A and porphyrin **3** were docked (**Figure 6**), it was clear that the presence of four enriched electrophilic benzoic functions properly approved the complementarity of compound **3**.

<**Figure 6**>

Two benzoic acid groups out of four in porphyrin **3**, expressed professional alignment extended out of the G-Q major groove. The other two benzoic acid substituents got extended back through the minor groove forming two distinctive hydrophilic and lipophilic interactions, respectively. A strong hydrogen bond was formed between DG13 and the benzoic carboxyl group and augmented the hydrophilic recognition of compound **3**. DG17 stabilized the phenyl group of the same benzoic function by expressing π-π stacking

interactions. Apparently, the ceiling DG-2 and DG-4 bases were recognized with π-π stacking with the heterocyclic pyrrole backbones (Fig. 7).

<Figure 7>

- Docking of compound 5

Docking of compound **5 showed** certain selectivity including the following features: **Firstly,** its global minima conformer identically aligned the POH-25A, the reference crystallographic ligand, and also the docked compound **3** (**Figure 8-A, B**). **Secondly**: Porphyrin **5** substituted with gigantic phenothiazine functions showed proper complementarity with G-quartet 2A5R protein. [**Figure 8-C**]. Compound **5** binds not only to the surrounding DG bases but also it performed four cation–π interactions with the phosphorous backbones namely DG5, DG14 and bifurcated two bonds out of DG13 (**Figure 8-D). Thirdly**, even there is no strong hydrogen bond between the phenothiazine ring and the G-Q bases, an overall π - π stacking hydrophobic interaction between DG8 and the heterocyclic phenothiazine ring is clearly exist

<Figure 8>

4   Conclusion:

A series of new porphyrin derivatives (**1–5**) have been synthesized in high yields (64-85%). Porphyrins **1** and **2** have been complexed successively with different metal salts such as Cu(II), VO^{2+}, Ag(I), Ni(II) and Pd(II), by one-pot mixed solvent method. The corresponding metalloporphyrins were obtained after 6–8 hours in high yield (> 80%). The relatively high yields obtained during the synthesis of the new porphyrins were attributed to the use of DMF as a capping agent for the pyrrole during the reaction. The newly

synthesized porphyrin derivatives are equipped with different aryl and heterocyclic substituents. The formation of the new compounds was confirmed by spectral and elemental analysis. The new compounds have been tested for their pharmacological activities. It can be concluded that the electronic properties of the peripheral substituents on the porphyrin moiety had a major effect on the antioxidant and cytotoxic activities. Compounds **4** and **2a** were the most powerful antioxidants due to the presence of hydroxyl groups in compound **4** and the dimethylamino donating group along with Cu(II) metal in complex **2a.** Porphyrin **1** showed the weakest antioxidant activity among all the newly synthesized porphyrins due to the presence of the electron withdrawing substituent (Cl). In general, porphyrins with electron donating groups showed stronger antioxidant activity than porphyrins equipped with electron withdrawing groups. In cytotoxicity tests, compounds **2**, **3** and **5** showed very strong activity towards both HePG2 and MCF-7 cell lines, while **1a, 1b, 2b** and **4** were only strong active antioxidant compounds for both cell lines due to the electronic effect of the substituent on the porphyrin moiety. Finally the molecular docking studies of the most powerful antioxidant derivatives (**2a** and **4**) and the most active antitumor (**3** and **5**) were carried out to explore their binding modes in the active sites of the studied proteins and results were reported. Compound **5** showed proper complementarity with G-quartet 2A5R protein, and therefore considered a promising, lead in the treatment of cancer

5   References

28

1. The porphyrin Handbook; Smith, K. M., Guilard, R, Eds; Academic Press: San Diego, 1999–2003, Vol. 1-20.

2. K. Suda, K, Baba, S. Nakajima, T. Takanami, *Chem Commun*., **2002**, 2570– 2572. doi: 10.1039/B207328E

3. D. Arteaga, R. Cotta, A. Ortiz, B. Insuasty, N. Martin, L. Echegoyen, *Dyes and Pigments*, **2015**, 112, 127–137. doi.org/10.1016/j.dyepig.2014.06.028

4. K. D. Seo, M. J. Lee, H. M. Song, H. S. Kang, H. K. Kim, *Dyes and Pigments*, **2012**, 94(1), 143–149. doi.org/10.1016/j.dyepig.2011.12.006

5. I. Hod, M. D. Sampson, P. Deria, C. P. Kubiak, O. K. Farha, J. T. Hupp, *ACS Catal.,* **2015**, 5(11), 6302–6309. doi.org/10.1021/acscatal.5b01767

6. Z.-C. Sun, Y.-B. She, Y. Zhou, X.-F. Song, K. Li, *Molecules*, **2011**, 16, 2960–2970.

7. Z. Xinhua, H. Jiesheng, S. Panwen, F. Yaoyu, *Polyhedron*, **1996**, 15(16), 2677–2679. doi.org/10.1016/0277-5387(95)00563-3

8. K. Kilian, M. Pegier, K. Pyrzynska, *Spectrochim. Act. A Mol. Biomol. Spectrosc*., **2016**, 159, 123–127. doi.org/10.1016/j.saa.2016.01.045

9. A. D. Alder, F. R. Longo, F. Kampas, J. Kim, *J. Inorg. Nucl. Chem.,* **1970**, 32(7), 2443–2445. doi.org/10.1016/0022-1902(70)80535-8

10. P. Rothemund, *J. Am. Chem. Soc.* **1936**, 58(4), 625–627. doi.org/10.1021/ja01295a027

11. P. Rothemund, *J. Am, Chem. Soc.* **1935**, 57(10), 2010–2011. doi.org/10.1021/ja01313a510

12. A. D. Alder, F. R. Longo, J. D. Finarelli, J. Goldmacher, J. Assour, L. Korsakoff, *J. Org. Chem.*, **1967**, 32(2), 476–476. doi:10.1021/jo01288a053

13. A. Kumar, S. Maji, P. Dubey, G. J. Abhilash, S. Pandey, S. Sarker, *Tetrahedron Lett.*, **2007**, 48(41), 7287–7290. doi.org/10.1016/j.tetlet.2007.08.046

14. Y. Chen, X. P. Zhang, *J. Org. Chem.*, **2003**, 68(11), 4432–4438. doi.org/10.1021/jo034063m

15. D. Holten, D. F. Bocian, J. S. Lindsey, *Acc. Chem. Res*., **2002**, 35(1), 57769. Doi:10.1021/ar970264z

16. D. F. O'Shea, M. A. Miller, H. Matsueda, J. S. Lindsey, *Inorg. Chem.*, **1996**, 35, 7325–7338. DOI:10.1021/ic960812p

17. A. A. Fadda, R. E. El-Mekawy, A. L. I. El-Shafei, H. Freeman, *Arch. Pharm*., **2013**, 346(1), 53–61. doi: 10.1002/ardp.201200313.

18. A. A. Fadda, R. E. El-Mekawy, A. El-Shafei, H. S. Freeman, D. Hinks, M. El-Fedawy, *J. Chem.*, **2013**, 11 pages. https://doi.org/10.1155/2013/340230

19. E. Tawfik, A, Fadda, N. N. Soliman, L. A. Abouzeid, A. Negm, *Journal of Porphyrins and Phthalocyanines*, **2019**, 23(3), 1–9. doi.org/10.1142/S1088424619500093

20. S. Mondal, K. Sahu, B. Patra, S. Jena, H. S. Biswal, S. Kar, *Dalton Trans.*, 2020, **49**, 1424–1432. DOI: 10.1039/C9DT03573G

21. S. M. A. Pinto, C. Henrique, V. A. Tome, C. S. Vinagreiro, M. J. F. Calvete, J. M. Dabrowski *et al., J. Porphyrins and Phthalocyanines*, **2016**, 20, 45–60. doi.org/10.1142/S1088424616300020
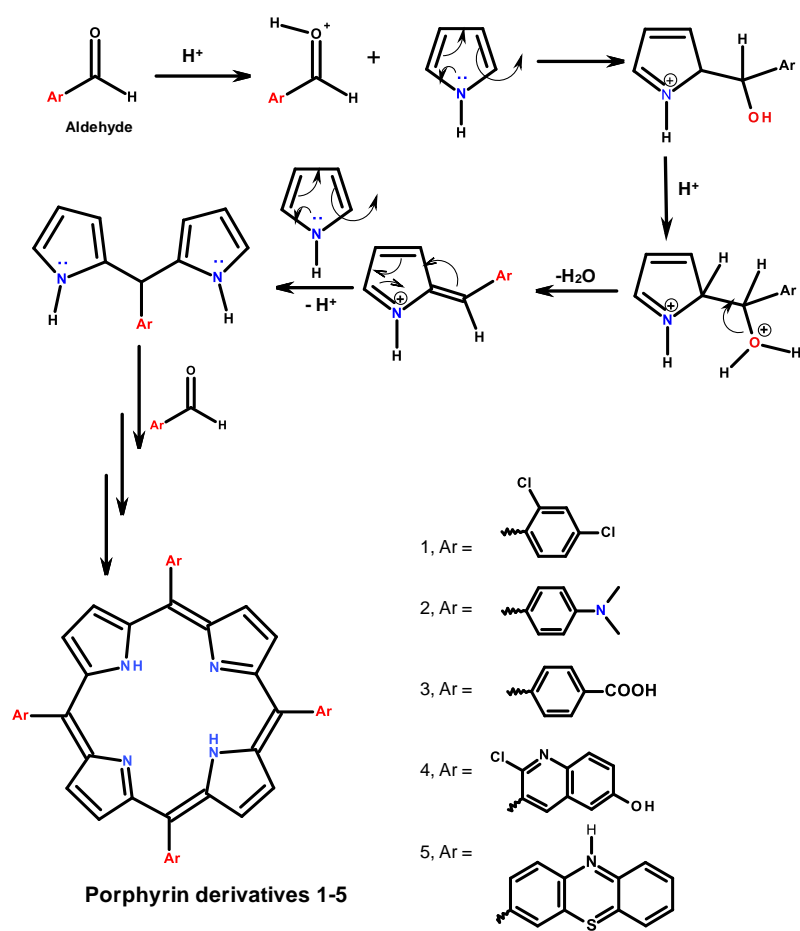
22. Q. Su, T. D. Hamilton, *Beilstein J. Org. Chem.* **2019,** *15,* 1149–1153. doi:10.3762/bjoc.15.111

23. J. C. Martinez, H. O. Garcia, L. E. Otheguy, G. S. Drummond, A. Kappas, *Journal of Perintology,* **2001**, 21, S101–S103. doi.org/10.1038/sj.jp.7210655

24. Q. Zhang, J. He, W. Yu, Y. Li, Z. Liu, B. Zhou, Y. Liu, *RSC Med. Chem.*, **2020**, Advance article. **https://doi.org/10.1039/C9MD00558G**

25. Satrialdi, R. Munechika, V. Biju, Y. Takano, H. Harashima, Y. Yamada, *Chem. Commun.*, **2020**, 56, 1145–1148. https://doi.org/10.1039/C9CC08563G

26. A. T. P. C. Gomes, M. G. P. M. S. Neves, J. A. S. Cavaleiro, *An. Acad. Bras. Cienc.* **2018**, 90, 993–1026. doi: 10.1590/0001-3765201820170811

27. X. Xue, A. Lindstrom, Y. Li, *Bioconjugate Chem.*, **2019**, 30(6), 1585–1603. doi: 10.1590/0001-3765201820170811

28. A. B. Ormond, H. S. freeman, *Dyes and Pigments*, **2013**, 96(2), 440–448. doi.org/10.1016/j.dyepig.2012.09.011

29. A. Garcia-Sampedro, A. Tabero, I. Mahamed, P. Acedo, Journal of Porphyrins and Phthaalocyanines, 2019, 23, 11–27. doi.org/10.1142/S1088424619500111

30. R. F. Barth, P. Mi, W. Yang, *Cancer Communications*, **2018**, 38(35), 1–15. https://doi.org/10.1186/s40880-018-0299-7

31. K. Hu, Z. Yang, L. Zhang, L. Xie, L. Wang, H. Xu, L. Josephson, S. H. Liang, M.-R. Zhang, *Coordination Chemistry Reviews*, **2020**, 405, 213139. https://doi.org/10.1016/j.ccr.2019.213139

32. T. J. Jensen, M. G. H. Vicente, R. Luguya, J. Norton, F. R. Fronczeck, K. M. Smith, *J. Photochem. Photobiol. B.*, **2010**, 100(2), 100–111. doi: 10.1016/j.jphotobiol.2010.05.007

33. K. A. D. F. Castro, N. M. M. Moura, F. Figueira, R. Ferreira, M. M. Q. Simoes, J. A. S. Cavaleiro, M. A. F. Faustino et al., *Int. J. Mol. Sci.*, **2019**, 29, 2522–2540. **https://doi.org/10.3390/ijms20102522**

34. E. Vaishnavi, R. Renganthan, *Analyst,* **2014**, 139, 225–234. doi.org/10.1039/C3AN01871G

35. A. N. Hurst, B. Scarbrough, R. Saleh, J. Hovey, F. Ari, S. Goyal, R. J. Chi et al., *Int. J. Mol. Sci.*, **2019**, 20, 134, 1–18. doi:10.3390/ijms20010134

36. I. A. Abdulaeva, K. P. Birin, J. Michalak, A. Roieu, C. Stern, A. Bessmertnykh-Lemeune, R. Guilard, Y. G. Gorbunova, A. Y. Tsivadze, *New J. Chem.*, **2016**, 40, 5758–5774. DOI: 10.1039/c5nj03247d

37. M. Luciano, C. Bruckner, *Molecules*, **2017**, 22, 980. doi:10.3390/molecules22060980

38. T. Fukuta, S. Hirai, T. Yoshida, T. Maoka, K. koqure, *Free Radical Research*, **2020**, in press. doi.org/10.1080/10715762.2019.1693042

39. J. Chen, J. Yang, L. Ma, J. Li, N. Shahzad, C. K. Kim, *Sci. Rep.,* **2020***,* 10**,** 2611. doi.org/10.1038/s41598-020-59451-z

40. J. Zhang, A. Wang, W. Zhao, C. Li, X, Chen, Y. Wang, W. Zhu, Q. Zhong, *Dyes and Pigments*, **2018**, 153, 241–247. https://doi.org/10.1016/j.dyepig.2018.02.028

41. W.-T. Chen, *Acta Cryst*., **2020**, 76, 133–138. doi.org/10.1107/S2053229619017273

42. F. Gutzeit, M. Dommaschk, N. Levin, A. Buchholz, E. Schaub, W. Plass, C. Näther, R. Herges, *Inorg. Chem.,* **2019**, 58, 19, 12542–12546. doi.org/10.1021/acs.inorgchem.9b00348
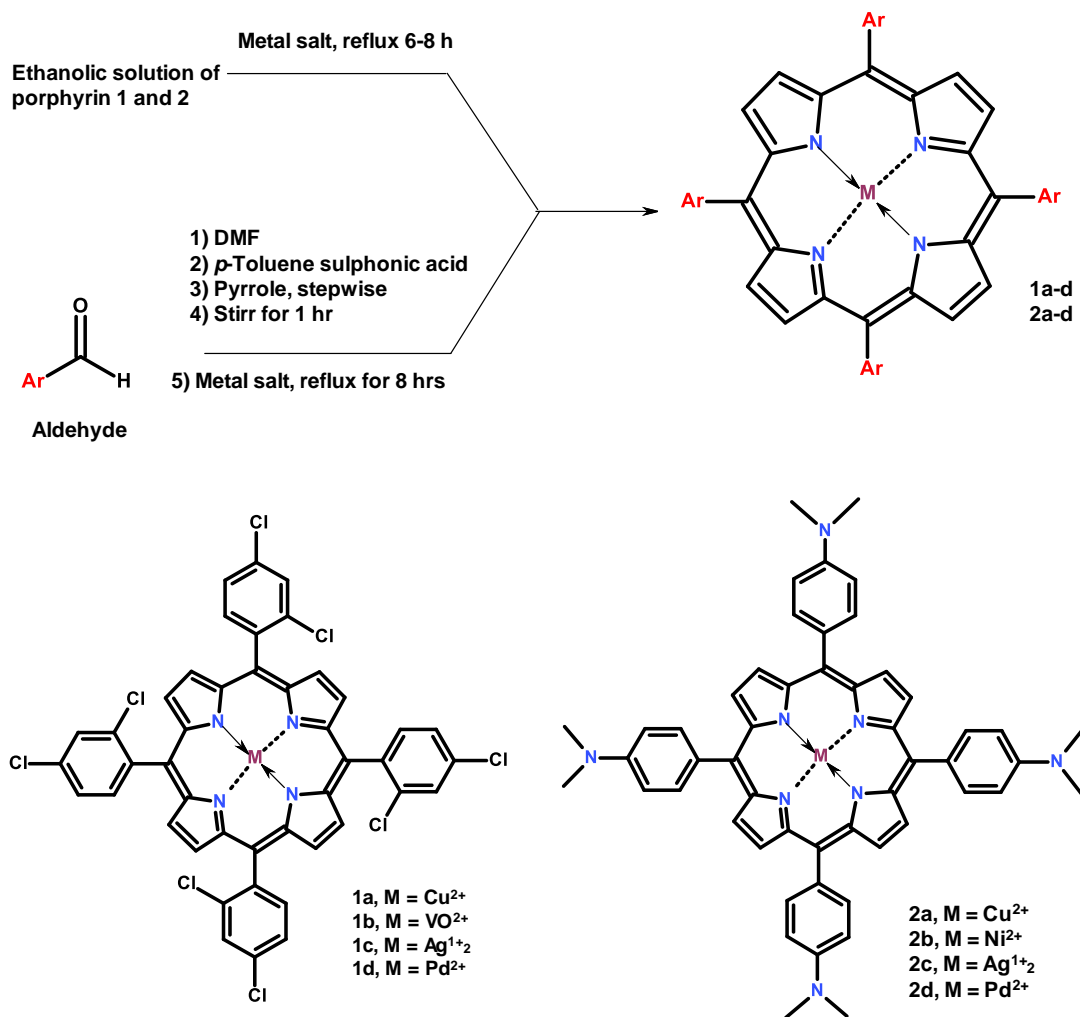
43. S. M. Shabangu, B. Babu, R. C. Soy, M. Managa, K. E. Sekhosana, T. Nyokong, *J. Coordination Chem.* **2020**, 73(4), 593–608.

https://doi.org/10.1080/00958972.2020.1739273

44. Schrödinger Relevsase 2019-3: Schrödinger Suite 2019-2 Protein Preparation Wizard; Epik, Schrödinger, LLC, New York, NY, 2019; Impact, Schrödinger, LLC, New York, NY, 2019; Prime, Schrödinger, LLC, New York, NY, 2019

45. P. Singh, R. Kumar, S. Tiwari, R. S. Khanna, A. K. Tewari, H. D. Khanna, *Clin Med Biochem,* **2015**, 1(105), 1–4. DOI: 10.4172/2471-2663.1000105

46. A. T. Phan, V. Kuryavyi, H. Y. Gaw, D. J. Patel, *Nat Chem Biol*., **2005**,1(3),167–73. DOI:10.1038/nchembio723

47. L. Boirre, G. Simonneaux, Y, Ferrand, S. Thibaut, Y. Lajat, T. Patrice, *J. Photochem. Photobiol. B*, **2003**, 69(3), 179–192. https://doi.org/10.1016/S1011-1344(03)00020-4

48. Y. Zhu, J, Chen, S. Kaskel, *Angew. Chem. Int. Ed*. **2020**, 10.1002, 1–25.

doi.org/10.1002/anie.201909880

49. E. Y. Tyulyaeva, *Russian Journal of Inorganic Chemistry***, 2019, 64**, 1775–1802. https://doi.org/10.1134/S0036023619140110

50. G. D. Bajju, Ashu, A. Ahmed, G. Devi, *BMC Chemistry*, **2019**, 13, 1–11. https://doi.org/10.1186/s13065-019-0523-9

51. Y. Kurumisawa, T. Higashino, S. Nimura, Y. Tsuji, H. Liyama, H. Imahori, *J. Am. Chem. Soc.* **2019**, 141, 25, 9910–9919. https://doi.org/10.1021/jacs.9b03302

52. A. Ungordu, Int J Quantum Chem. 2020,120:e26128. DOI: 10.1002/qua.26128

53. K. R. Oslon, Y. Gao, F. Arif, S. Patel, X. Yuan, V. Mannam, et al. *Antioxidants* **2019**, *8*(12), 639–657. **https://doi.org/10.3390/antiox8120639**

54. H. M. Ahn, J. M. Bae, M. J. Kim, K. H. Bok, H. Y. Jeong, S. J. Lee, C. Kim, Chem. Eur.J., 2017, 23,11969 –11976. **doi.org/10.1002/chem.201702750**

55. A. S. Munde, A. N. Jagdale, S. M. Jadhav, T. K. Chondhekar, Journal of the Korean Chemical Society, 2009, 53(4), 407–414. doi.org/10.5012/jkcs.2009.53.4.407

56. Z. Biyiklioglu, H. Kantekin, M. Ozil, Organomet. Chem. 2007, 692, 2436–2440. https://doi.org/10.1016/j.jorganchem.2007.02.013

57. Z. Valicsek, O. Horvath, Microchemical Journal, 2013, 107,47–62. DOI: 10.1016/j.microc.2012.07.002

58. M. Nakamura, K. Kawai, Y. Fujiwara, J. Catalysis, 1974, 34(3), 345–355. https://doi.org/10.1016/0021-9517(74)90047-5

59. B. T. Thaker, J. Lekhadia, A. Patel, P. Thaker, *Transition Metal Chemistry*, 1994, **19**, 623–631. https://doi.org/10.1007/BF00980417

60. S. Khasa, V. P. Seth, P. S. Gahlot. A. Agarwal, R. M. Krishna, S. K. Gupta, 2003, Physica B, 334, 347–358. doi:10.1016/S0921-4526(03)00097-8

61. N. Raman, A. Kulandaisamy, C. Thangaraja, K. Jeyasubramanian, 2003, *Transition Metal Chemistry* **volume 28**, pages29–36. doi.org/10.1023/A:1022544126607

62. U. Al-Ayaan, I. M. Gaber, *Spectrochim. Acta Part A: Mol. Biomol. Spectroscopy*, **2007**, 67(1), 263–272. https://doi.org/10.1016/j.saa.2006.07.012

63. A. Braca, C. Sortino, I, Morelli, J. Mendez, **Journal of Ethnopharmacology, 2002,** 79(3), 379–381. DOI: 10.1016/s0378-8741(01)00413-5

64. M. Szelag, D. Milkulski, M. Molski, *J Mol Model*., **2012**, 18(7), 2907–2916. doi: 10.1007/s00894-011-1306-y

65. I. P. Ejidike, P. A. Ajibade, *Bioinorg. Chem. Appl.,* **2015**, 2015, 1–9. https://doi.org/10.1155/2015/890734

66. C. Y. Lee, C. N. Nanah, R. A. Held, A. R. Clark, U. G. Huynh, M. C. Maraskine et al., *Biochimie*, **2015**, 111:125–134. doi: 10.1016/j.biochi.2015.02.001

67. N. M. Aburas, N. R. Stevanovic, M. K. Milcic, A. D. Lolic, M. M. Natic, Z. Lj. Tesic, R. M. Baosic, *J. Braz. Chem. Soc*., **2013**, 24, 1322–1328. doi.org/10.5935/0103-5053.20130167

Scheme 1. Synthetic route for the preparation of porphyrin derivatives 1–5.

Metal salt, reflux 6-8 h

Ethanolic solution of
porphyrin 1 and 2

1) DMF
2) *p*-Toluene sulphonic acid
3) Pyrrole, stepwise
4) Stirr for 1 hr

5) Metal salt, reflux for 8 hrs

Aldehyde

1a-d
2a-d

1a, M = Cu^{2+}
1b, M = VO^{2+}
1c, M = Ag^{1+}_2
1d, M = Pd^{2+}

2a, M = Cu^{2+}
2b, M = Ni^{2+}
2c, M = Ag^{1+}_2
2d, M = Pd^{2+}

Scheme 2. The synthetic routes for metal porphyrin complexes **1a–d** and **2a–d**
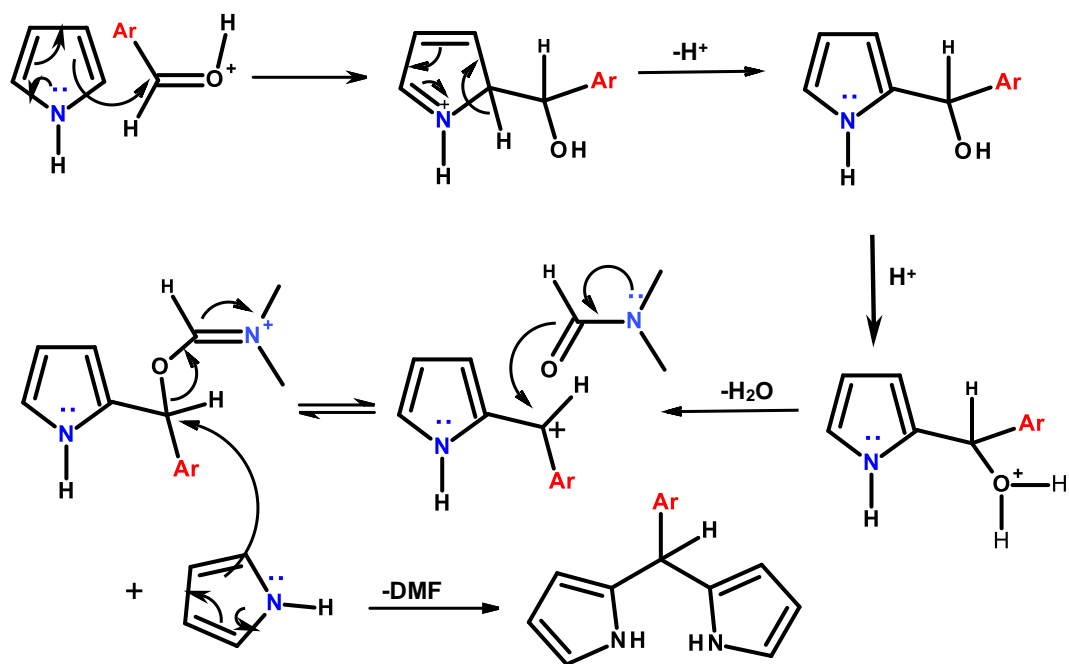
Scheme 3: Proposed reaction mechanism shows capping mechanism for the synthesis of porphyrin derivatives **1–5, 1a–d** and **2a–d** showing how DMF acts as a good leaving group as pyrrole added [17]

Tables

Table 1: Inhibitive concentration (IC50) and inhibition % values of the antioxidant activity of the investigated compounds.

Compound no.	IC_{50} (mg/ mL)	% Inhibition at 0.002 mg/ mL	% Inhibition at 0.005 mg/ mL	% Inhibition at 0.01 mg/ mL
1	1.760	54.43	56.11	58.40
2	0.313	65.42	70.69	--
3	0.718	60.84	67.10	--
4	0.015	--	--	--
5	0.125	75.28	--	--
1a	0.239	70.69	71.80	80.0
1b	0.203	69.99	72.95	--
1c	0.501	59.08	63.59	73.82
1d	0.346	64.05	69.27	75.73
2a	0.004	--	--	--
2c	0.155	75.24	76.05	83.40
2d	0.162	74.96	75.95	82.44
Vit. C	0.022	--	--	--

Table 2. Cytotoxicity (IC_{50}) of tested compounds on different cancer cell lines

IC$_{50}$ (mg/ ml): 1-10 (very strong), 11-25 (strong), 26-50 (moderate), 51-100 (weak), 100-200 (very weak), 200 (noncytotoxicity)

Compounds	Cytotoxicity IC$_{50}$ ($\mu g/mL$)	
	HePG-2	MCF-7
Doxorubicin	4.5±0.3	4.17±0.2
1	27.08±2.2	20.89±1.7
1a	12.90±2.6	19.37±1.6
1b	18.31±3.1	21.02±2.8
1c	51.32±3.8	60.54±3.9
1d	48.49±4.3	55.33±4.5
2	5.52±1.1	5.83±1.2
2a	28.26±3.2	31.12±3.7
2b	18.71±1.7	16.43±2.0
2c	31.65±2.9	29.50±2.6
2d	51.86±3.6	44.61±3.2
3	6.34±0.7	7.51±0.5
4	14.81±1.5	15.38±1.3
5	5.56±0.4	4.28±0.3
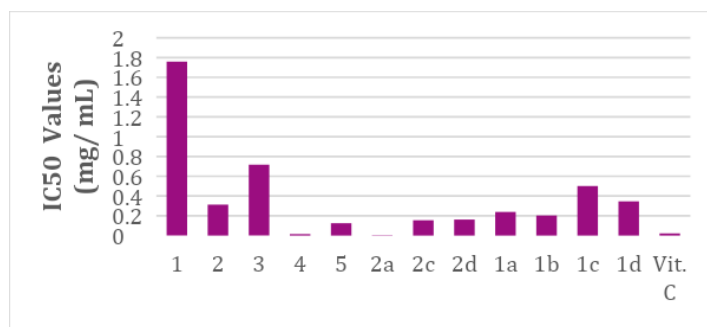
Figure 1. Comparison of the IC$_{50}$ values of the tested compounds.
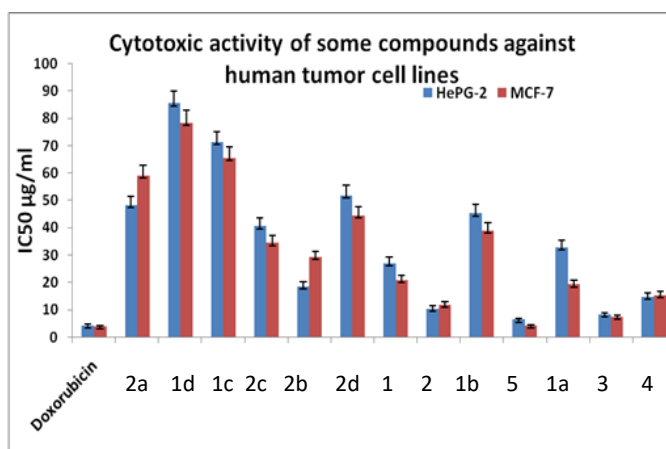
Figure 2: IC$_{50}$ values in µg/mL of the compounds from MTT viability assays of HepG-2 and MCF-7 cell lines.
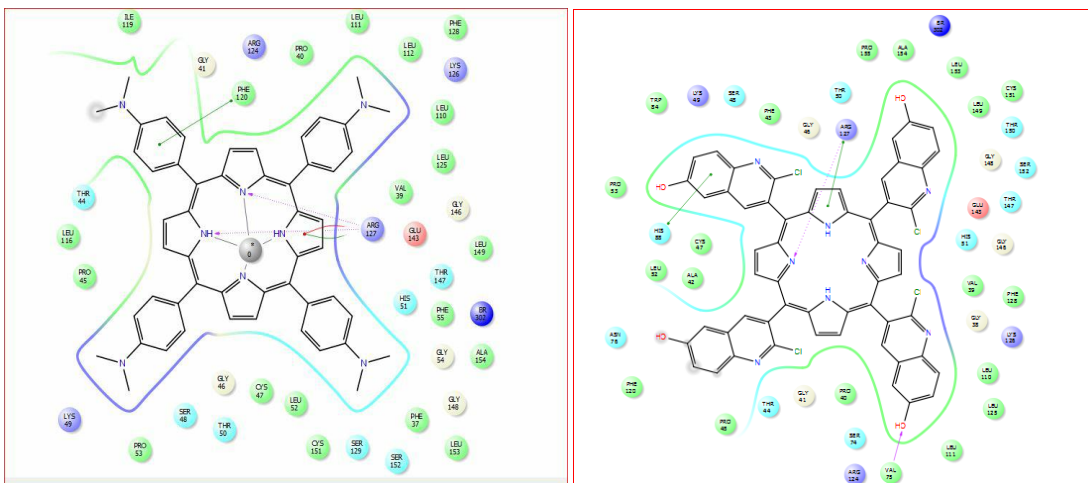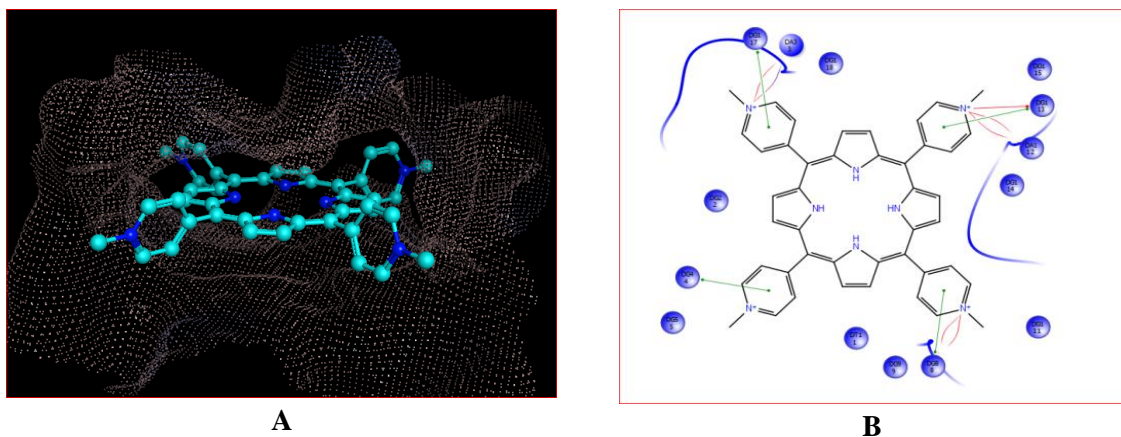

Figure 3: Docking of Compounds 2a & 4

Figure 4: **A**: 2-D chemical structure of ligand **POH 25A** that was in complex of DNA Tetraplex (PDB code 2A5R).

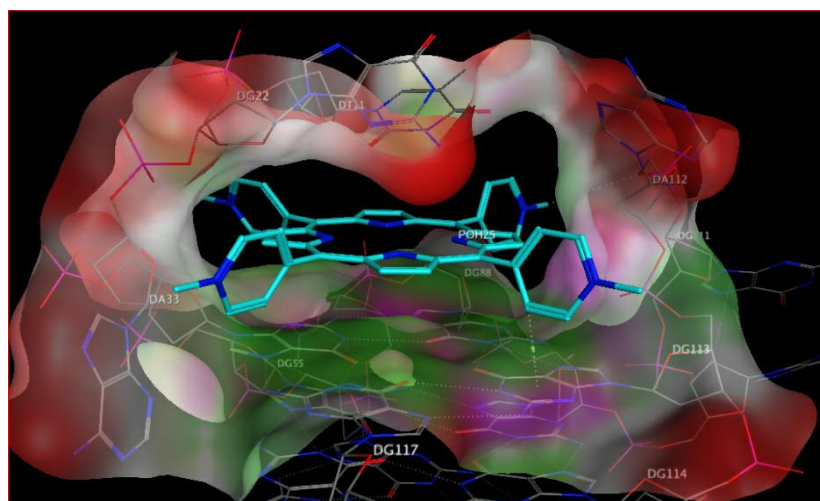**B**: the 2-D docking of **POH 25A at the major groove of G-**quartet DNA.

Figure 5: 3-D crystallographic interaction of ligand **POH 25A** that was in complex of G-quartet DNA (PDB code 2A5R).
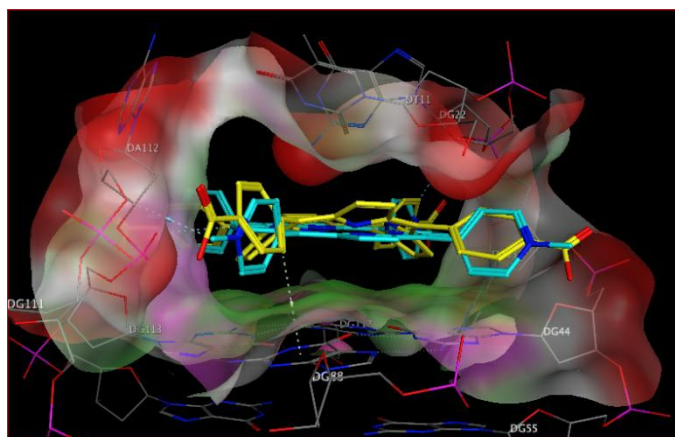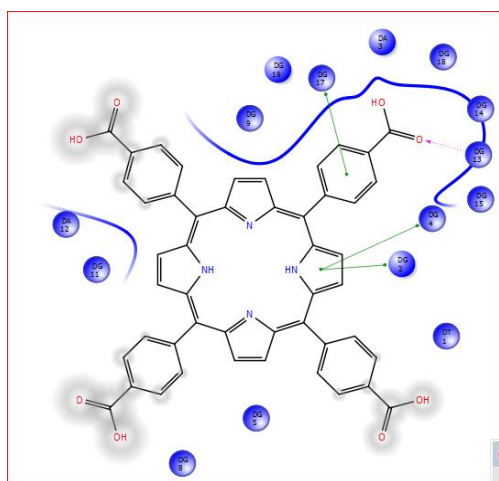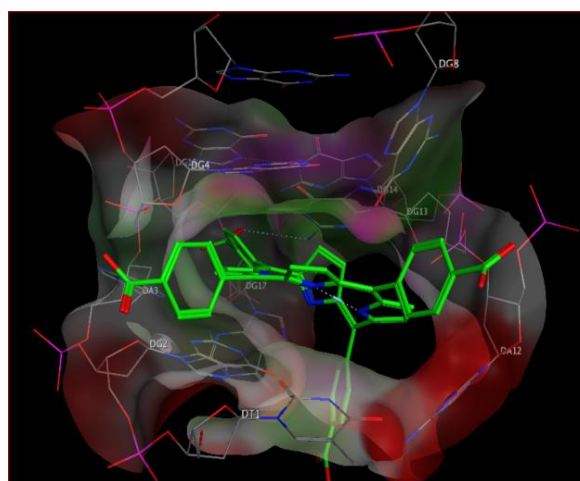
Figure 6: Comparative docking studies of POH 25A with porphyrin-**3**

| A | B |

Figure 7: **A**: The 2-D docking of POH 25A at the major groove of G-quartet DNA.
B: 3-D crystallographic interaction of ligand **POH** 25A that was in complex of G-quartet DNA
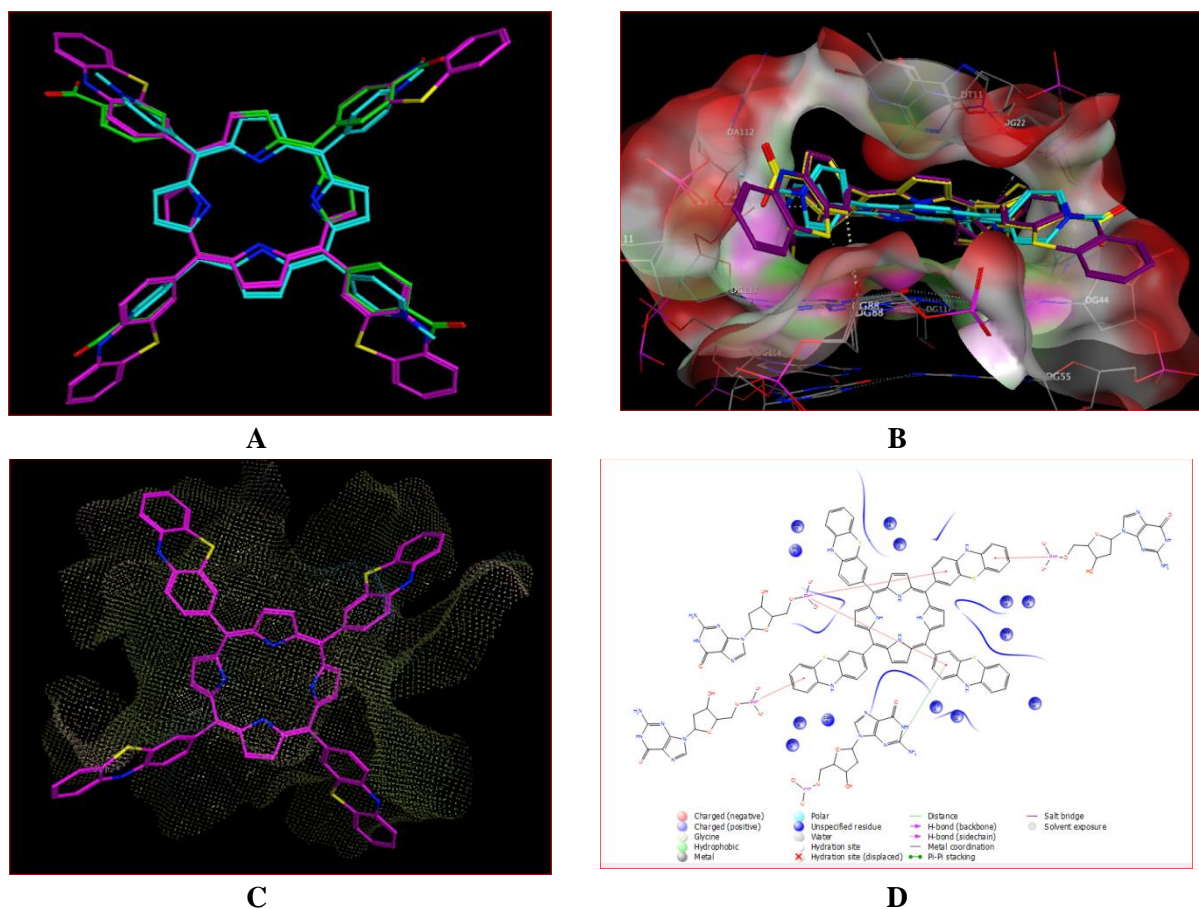(PDB code 2A5R).

A

B

C

D

Figure 8: A) 2-D molecular structure of alignment of 2A5R docked ligand (cyano), compound 3 (green) and 5 (purple).

B) 3-D molecular surface structure of aligned ligands namely POH25A, (cyano), compound **3** (green) and **5** (purple).

C) Porphyrin 5 substituted with gigantic phenothiazine functions showed proper complementarity with G-quartet 2A5R protein.

D) Cation–π interactions with the phosphorous backbones namely DG5, DG14 and bifurcated two bonds out of DG13